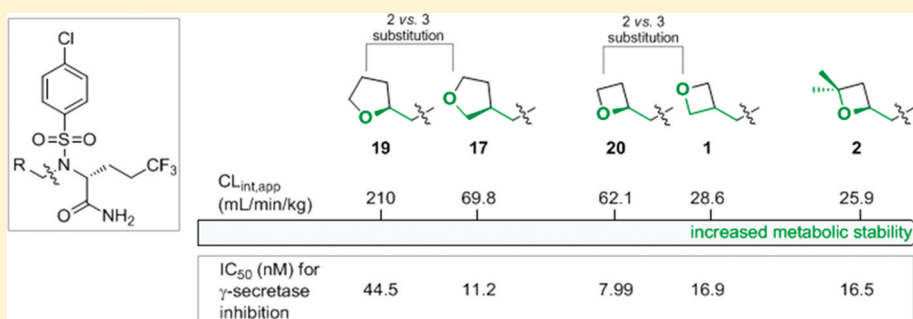


Metabolism-Directed Design of Oxetane-Containing Arylsulfonamide Derivatives as γ -Secretase Inhibitors

Antonia F. Stepan,* Kapil Karki, W. Scott McDonald, Peter H. Dorff, Jason K. Dutra, Kenneth J. DiRico, Annie Won, Chakrapani Subramanyam, Ivan V. Efremov, Christopher J. O'Donnell, Charles E. Nolan, Stacey L. Becker, Leslie R. Pustilnik, Blossom Sneed, Hao Sun, Yasong Lu, Ashley E. Robshaw, David Riddell, Theresa J. O'Sullivan, Evelyn Sibley, Steven Capetta, Kevin Atchison, Andrew J. Hallgren, Emily Miller, Anthony Wood, and R. Scott Obach

Pfizer Worldwide Research & Development, Eastern Point Road, Groton, Connecticut 06340, United States

Supporting Information



ABSTRACT: A metabolism-based approach toward the optimization of a series of *N*-arylsulfonamide-based γ -secretase inhibitors is reported. The lead cyclohexyl analogue **6** suffered from extensive oxidation on the cycloalkyl motif by cytochrome P450 3A4, translating into poor human liver microsomal stability. Knowledge of the metabolic pathways of **6** triggered a structure–activity relationship study aimed at lowering lipophilicity through the introduction of polarity. This effort led to several tetrahydropyran and tetrahydrofuran analogues, wherein the 3- and 4-substituted variants exhibited greater microsomal stability relative to their 2-substituted counterparts. Further reduction in lipophilicity led to the potent γ -secretase inhibitor and 3-substituted oxetane **1** with a reduced propensity toward oxidative metabolism, relative to its 2-substituted isomer. The slower rates of metabolism with 3-substituted cyclic ethers most likely originate from reductions in lipophilicity and/or unfavorable CYP active site interactions with the heteroatom. Preliminary animal pharmacology studies with a representative oxetane indicate that the series is generally capable of lowering $A\beta$ in vivo. As such, the study also illustrates the improvement in druglikeness of molecules through the use of the oxetane motif.

INTRODUCTION

Alzheimer's disease (AD) is the most prevalent form of senile dementia in the elderly population.¹ Current treatment options are only symptomatic, and thus, disease-modifying anti-Alzheimer's drugs that slow or reverse neuronal loss and the underlying cognitive decline are urgently needed. Histopathological and genetic evidence suggests that the formation of the amyloid- β ($A\beta$) peptide and its subsequent aggregation to oligomers and plaques are key events in disease progression.² $A\beta$ peptides are produced by sequential proteolytic cleavage of the $A\beta$ precursor protein by two aspartyl proteases, β - and γ -secretases.³ Heterologous cleavage by γ -secretase creates $A\beta$ isoforms ranging from 37 ($A\beta_{37}$) to 42 ($A\beta_{42}$) amino acid residues. $A\beta_{40}$ is the most abundant isoform, while it is thought that $A\beta_{42}$ is closely associated with the pathogenesis of AD. As a result, reduction in the formation of $A\beta$ peptides via inhibition of γ -secretase by small molecule agents appears to be a viable option for the treatment of AD. Because of the role of

γ -secretase in Notch processing,^{4,5} identification of inhibitors with minimal impact on Notch signaling is an important consideration from a drug discovery perspective. Indeed, a number of structurally diverse γ -secretase inhibitors with Notch-sparing activity have been reported in the primary literature,⁶ and several (e.g., BMS-708,163, LY-450,139, GSI-953, PF-3,084,014, and BMS-299,897) have also advanced into clinical trials for the treatment of AD (Figure 1).⁷

As part of ongoing efforts to identify novel chemotypes,^{6k,l} we report our structure–activity relationship (SAR) findings on a series of *N*-substituted arylsulfonamides as potent γ -secretase inhibitors. The incorporation of in vitro metabolite identification studies in human hepatic tissue at the lead optimization stage greatly facilitated our efforts in the modulation of physicochemical property space and led to the rational design

Received: July 7, 2011

Published: October 13, 2011

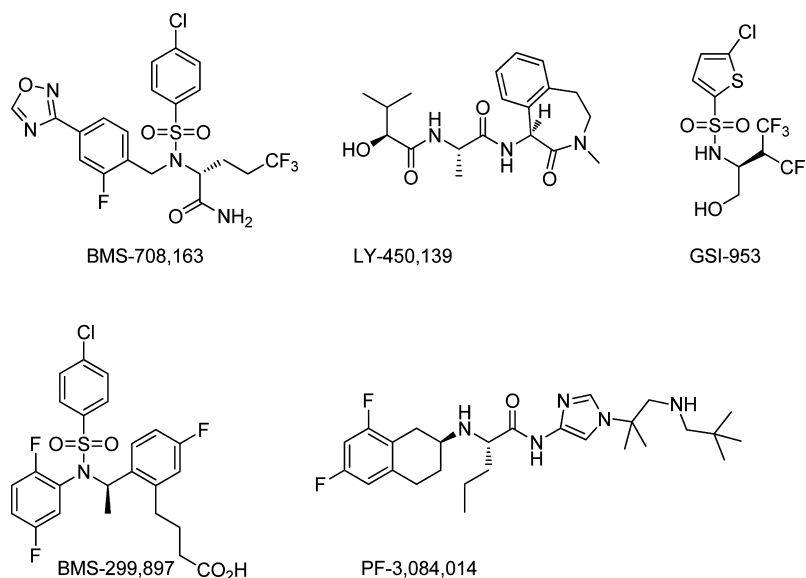


Figure 1. γ -Secretase inhibitors in clinical trials.

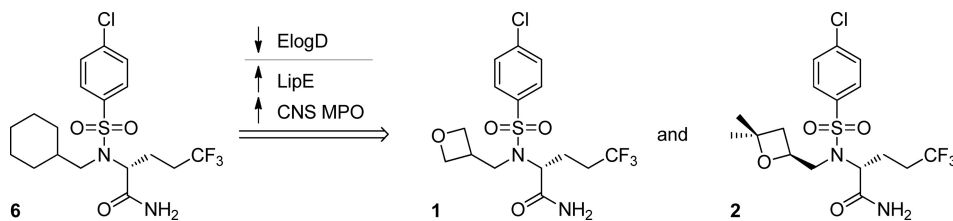
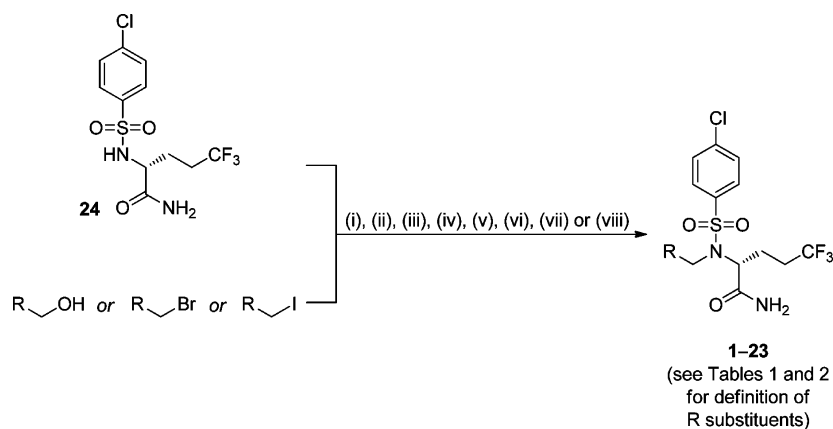


Figure 2. Design progression toward compounds 1 and 2.

Scheme 1. Synthesis of Compounds 1–23^a



^aReagents and conditions: (i) (Oxetan-3-yl)methanol (for 1)/(tetrahydrofuran-3-yl)methanol (for 16 and 17)/(tetrahydrofuran-2-yl)methanol (for 18 and 19)/(oxetan-2-yl)methanol (for 20 and 21), DEAD, PPh₃, THF, 23 °C. (ii) Cyclohexylmethanol (for 6)/cyclopentylmethanol (for 7)/cyclobutylmethanol (for 8), DCAD, PPh₃, THF, 23 °C. (iii) (a) (Bromomethyl)tetrahydro-2H-pyran (for 9 and 10), Cs₂CO₃, DMF, 80 °C. (iv) (a) (Tetrahydro-2H-pyran-3-yl)methanol (for 11 and 12)/(S)-(1,4-dioxan-2-yl)methanol (for 15)/(R)-(1,4-dioxan-2-yl)methanol (for 14), CH₃SO₂Cl, NEt₃, CH₂Cl₂, 0 °C then 24, Cs₂CO₃, DMF, 80 °C. (v) 4-(Iodomethyl)tetrahydro-2H-pyran, Cs₂CO₃, DMF, 80 °C. (vi) Compound 25, Cs₂CO₃, DMAc, 60 °C. (vii) Compound 26, Cs₂CO₃, DMAc, 90 °C. (viii) (3,3-Dimethyloxetan-2-yl)methanol, DBAD, PPh₃, THF, 23 °C, 16 h.

of oxetane derivatives 1 and 2 (Figure 2) with potent γ -secretase inhibitory activity, Notch selectivity, and superior oxidative metabolic stability. A prominent highlight of the SAR studies was the discovery of the oxetane ring system with the appropriate balance of potency, metabolic stability, and permeability, relative to simple cycloalkyl rings and other cyclic ethers. These observations are compatible with the recent reports by Carreira and co-workers, which highlight the

attractive physicochemical and disposition attributes of the oxetane functionality in drug design.⁸

RESULTS AND DISCUSSION

Chemistry. Title compounds 1–23 were prepared via alkylation of sulfonamide 24^{7c} with the appropriate alkyl alcohol or alkyl halide (Scheme 1). In the case of several cyclic ethers, the alkylation products were obtained as diastereomeric

Table 1. In Vitro Pharmacology and Disposition Data for a Representative Set of *N*-Arylsulfonamides

Compound	R	IC ₅₀ (Aβ ₄₂ , nM) ^{a,b}	Notch select- ivity	CL _{int,app} (mL/min/kg) ^{b,c}	ElogD ^d	RRCK <i>P</i> _{app} (A to B) (10 ⁻⁶ cm/s) ^e	MDR1/MD CK BA/AB ^f
6		12.3 (4)	n.d.	176 (3)	5.60	4.42	1.99
7		16.6 (4)	160	229 (2)	5.15	6.01	1.70
8		11.7 (7)	171	207 (4)	4.67	11.1	1.58
9^g		7.97 (3)	298	>300 (2)	4.30	13.4	1.33
10^g		27.9 (3)	129	>300 (2)	4.30	15.4	1.16
11^g		33.8 (5)	123	156 (3)	3.60	18.2	1.77
12^g		45.2 (5)	103	136 (2)	3.70	18.4	1.46
13		8.58 (6)	412	114 (5)	3.50	26.3	1.69
14		5.25 (5)	856	117 (3)	2.75	27.3	1.71
15		7.53 (4)	420	176 (3)	2.75	20.6	1.47
18^g		5.51 (3)	n.d.	231 (3)	3.60	19.1	1.46
19^g		44.5 (4)	n.d.	210 (2)	3.50	22.4	1.37
16		13.4 (4)	457	83.4 (3)	2.80	21.7	1.50
17		11.2 (4)	363	69.8 (3)	2.80	20.5	1.71

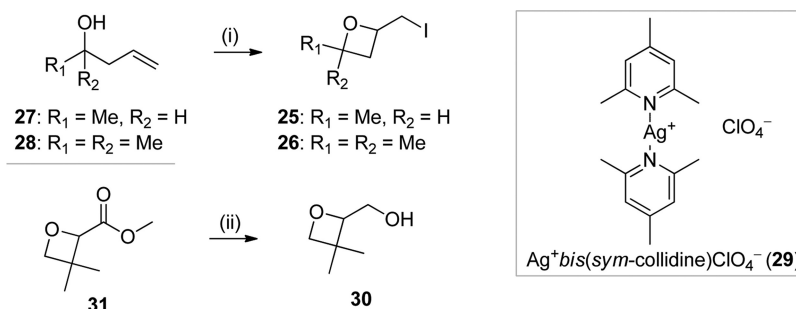
mixtures, which were separated chromatographically to afford the individual stereoisomers (Table 1). The alkyl alcohols and alkyl iodides required for the synthesis of compounds 2–5 were

not commercially available and were prepared as outlined in Scheme 2. Iodo-containing oxetanes **25** and **26** were prepared via an iodocyclization of homoallylic alcohols **27** and **28** using

Table 1. continued

Compound	R	IC ₅₀ (Aβ ₄₂ , nM) ^{a,b}	Notch select- ivity	CL _{int,app} (mL/min/kg) ^{b,c}	ElogD ^d	RRCK P _{app} (A to B) (10 ⁻⁶ cm/s) ^e	MDR1/MD CK BA/AB ^f
20		7.99 (4)	523	62.1 (14)	2.60	34.9	1.73
21		16.4 (3)	n. d.	63.8 (13)	2.60	28.7	1.26
1		16.9 (3)	187	28.6 (13)	2.50	25.4	1.99

^aIC₅₀ values were obtained in a whole cell assay using hu APP_{wt} cells by measuring Aβ₁₋₄₂ as previously described.¹² ^bNumber of repetitions indicated in parentheses. ^cCL_{int,app} refers to total intrinsic clearance obtained from scaling in vitro HLM half-lives. ^dElog D was measured at pH 7.4 as previously described.¹³ ^eRRCK cells with low transporter activity were isolated from Madine–Darby canine kidney cells and were used to estimate intrinsic absorptive permeability.¹⁴ ^fMDR1/MDCK assay utilized MDCK cells transfected with the gene that encodes human *p*-glycoprotein.¹⁴ ^gThe absolute configuration was arbitrarily assigned.

Scheme 2. Synthesis of Substituted Oxetanes 25, 26, and 30^a

^aReagents and Conditions: (i) Ag⁺(sym-collidine)ClO₄⁻ (29), I₂, 23 °C, CH₂Cl₂, 16 h. (ii) LiAlH₄, THF, -30 °C, 1.5 h.

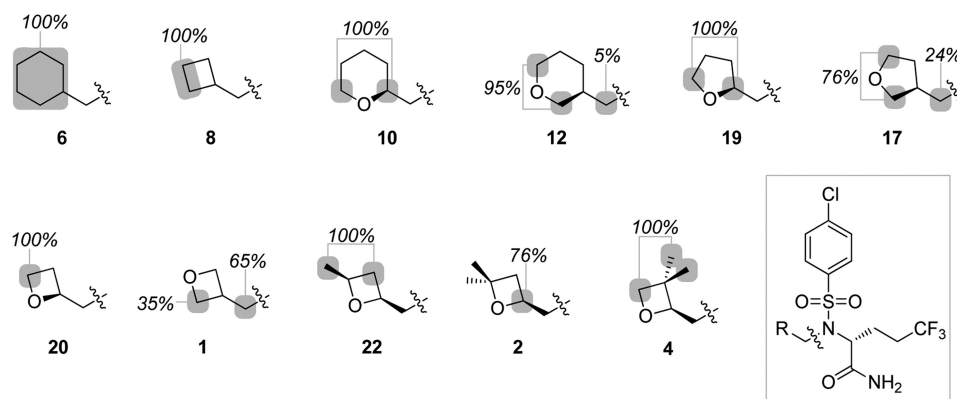


Figure 3. Sites of oxidative metabolism in HLM for representative *N*-arylsulfonamides.

the I⁺ transfer reagent bis(sym-collidine)iodine perchlorate, generated in situ from silver bis(sym-collidine)iodine perchlorate (29) and iodine.⁹ The crude products obtained in these reactions were used in the alkylation step without further purification. 3,3-(Dimethyl-oxetan-2-yl)methanol (30) was accessed from known ester 31¹⁰ via reduction to the corresponding alcohol.

In Vitro Pharmacology and Metabolism SAR. The starting point of our study was the identification of compound 6 (Figure 2), obtained by replacement of the biaryl core in BMS-708,163 with a smaller cyclohexyl group.¹¹ Although 6

demonstrated good γ -secretase inhibition [IC₅₀ (Aβ₄₂) = 12.3 nM, Table 1] in our whole cell assay,¹² the compound suffered from high oxidative metabolic turnover in human liver microsomes (HLM; apparent intrinsic clearance, CL_{int,app} = 176 mL/min/kg), a phenomenon that is likely related to the lipophilic nature of the molecule (Elog D = 5.60).¹³ In addition to its metabolic instability, the moderate permeability of 6 (P_{app} = 4.42 × 10⁻⁶ cm/s) in the RRCK assay¹⁴ indicates that the compound might suffer from poor oral bioavailability.

Replacement of the cyclohexane ring in 6 with smaller cycloalkyl rings (compounds 7 and 8) had minimal effect on γ -

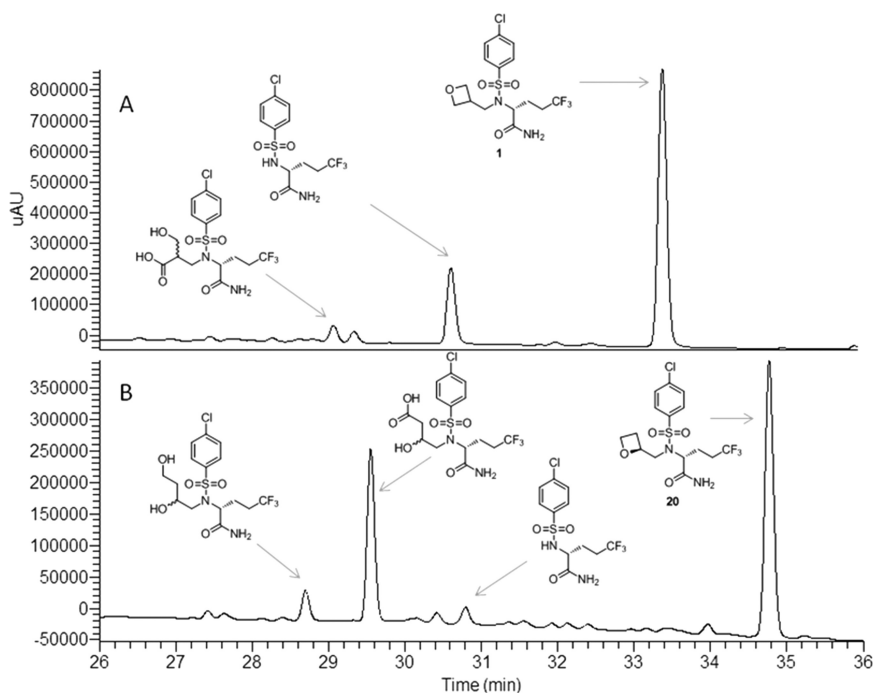


Figure 4. HPLC-UV chromatograms of metabolites of compounds **1** (A) and **20** (B) in NADPH-supplemented HLM.

secretase potency [IC_{50} ($A\beta_{42}$) = 16.6 and 11.7 nM] but, unfortunately, did not improve the metabolic liability ($CL_{int,app}$ = 229 and 207 mL/min/kg). To elucidate the source(s) of the metabolic instability in the cycloalkyl derivatives, the biotransformation pathways of representative members **6** and **8** were examined in NADPH-supplemented HLM. The formation of multiple cytochrome P450 (CYP)-mediated hydroxylated metabolites derived exclusively from oxidations of the cycloalkyl moiety was noted for both compounds (Figure 3). No metabolism was discerned on the aryl chloride or trifluoropropane substituents in compounds **6** and **8**, respectively.

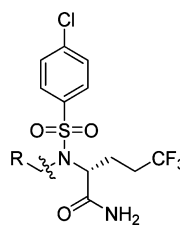
With the source of metabolic instability identified, we decided to introduce polarity into the cycloalkyl ring system as a tactic to potentially reduce oxidative metabolism, while retaining pharmacologic activity. As illustrated with compounds **9–19**, incorporation of oxygen into the cycloalkyl ring system reduced Elog *D* but did not substantially impact γ -secretase inhibitory potency noted with **6**, suggesting that the overall approach was a viable one to reduce HLM clearance. Of much interest in this SAR study was the finding that the 3- and 4-substituted tetrahydropyran analogues **11–13** displayed greater resistance toward oxidative metabolism in HLM as judged by a greater than 2-fold decrease in $CL_{int,app}$ relative to the 2-substituted tetrahydropyran counterparts (compounds **9** and **10**). A similar trend with respect to HLM stability was also noted with the 3-substituted tetrahydrofurans (compounds **16** and **17**) relative to the 2-substituted derivatives (compounds **18** and **19**). Compound **14** displayed a greater than 2-fold improvement in γ -secretase inhibition [IC_{50} ($A\beta_{42}$) = 5.25 nM], relative to lead compound **6** [IC_{50} ($A\beta_{42}$) = 12.3 nM]. However, metabolic turnover in HLM remained relatively high ($CL_{int,app}$ = 117 mL/min/kg), despite a net reduction in ELog *D* value as compared with **6**.

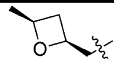


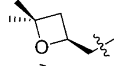
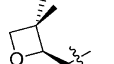

To gain an insight into the biochemical basis for the greater metabolic resistance of 3-substituted cyclic ethers as opposed to the 2-substituted analogues, additional metabolite identification

studies were performed in HLM with representative members of the 2- and 3-substituted tetrahydropyrans (compounds **10** and **12**) and tetrahydrofurans (compounds **17** and **19**). As seen in Figure 3, oxidative metabolism on all compounds still occurred primarily on the cycloether ring. For the tetrahydropyran and tetrahydrofuran rings, the characterization of stable hydroxy-carboxylic acid metabolites is consistent with an initial CYP-catalyzed oxidation(s) on the carbon α to the oxygen atom, which would lead to unstable hemiacetal intermediates followed by hydrolysis to the corresponding aldehyde derivatives and further oxidation to the corresponding hydroxy-acid metabolites. On the basis of these observations, we speculate that the greater stability of the 3-substituted cyclic ethers (relative to the 2-substituted variants) results from a slower overall rate of metabolism caused by a diminished affinity for CYP binding due to a reduction in Elog *D* and/or unfavorable active site interactions with the 3-oxo substituent. It is possible that net reductions in Elog *D* values for the 3-substituted cyclic ethers arises from a greater degree of solvation of the more exposed oxygen atom in the 3-substituted cyclic ethers (relative to the 2-substituted analogues).

Encouraged by these findings, we decided to further investigate whether such metabolic differences could be preserved with the even less lipophilic oxetane ring system. We were pleased to find out that, relative to the other cyclic ethers, the oxetane-containing sulfonamides (compounds **20**, **21**, and **1**) possessed the highest degree of HLM stability, while retaining γ -secretase inhibitory potency in the low nanomolar range. While the increased metabolic stability is most likely a reflection of reduced lipophilicity [Elog *D* = 2.50–2.60 (compounds **1**, **20**, and **21**)], there is a distinct possibility that the greater chemical stability of the oxetane ring (relative to the higher cyclic ether homologues) in **20**, **21**, and **1** also induces metabolic resistance. Certainly, using *tert*-butoxyl radicals, it has been demonstrated that the rate of hydrogen abstraction α to oxygen atoms is lower in oxetanes relative to tetrahydrofurans and tetrahydropyrans.¹⁵

Table 2. In Vitro Pharmacology and Disposition Data for Substituted Oxetanes



Compound	R	IC ₅₀ (Aβ ₄₂ , nM) ^{a,b}	Notch selectivity	CL _{int,app} (mL/min/kg) ^{b,c}	ElogD ^d	RRCK ^e (10 ⁻⁶ cm/s) ^e	MDR1/MDCK BA/AB _{corr} ^f
22 ^g		10.8 (3)	n. d.	167 (3)	3.40	21.8	1.49
23 ^g		6.46 (3)	n. d.	76.9 (3)	3.40	21.2	1.57
3 ^h		72.4 (3)	129	29.0 (2)	3.80	18.1	1.32
2 ^h		16.5 (3)	439	25.9 (13)	3.80	14.9	1.04
4 ^h		49.0 (3)	151	>293 (3)	3.90	22.3	1.78
5 ^h		49.5 (3)	171	262 (13)	3.80	26.4	1.51

^aIC₅₀ values were obtained in a whole cell assay using hu APP_{wt} cells by measuring Aβ₁₋₄₂ as previously described.¹² ^bNumber of repetitions indicated in parentheses. ^cCL_{int,app} refers to total intrinsic clearance obtained from scaling in vitro HLM half-lives. ^dElog *D* was measured at pH 7.4 as previously described.¹³ ^eRRCK cells with low transporter activity were isolated from MDCK cells and were used to estimate intrinsic absorptive permeability.¹⁴ ^fMDR1/MDCK assay utilized MDCK cells transfected with the gene that encodes human *p*-glycoprotein.¹⁴ ^gThe relative configuration was assigned using a set of two-dimensional NMR spectroscopy experiments (COSY and NOE); the absolute configuration was arbitrarily assigned. ^hThe absolute configuration was arbitrarily assigned.

The relationship between oxetane ring substitution and oxidative metabolic stability followed similar trends as seen with the tetrahydropyran and tetrahydrofuran derivatives. Thus, 3-substituted oxetane **1** (CL_{int,app} = 28.6 mL/min/kg) was relatively more stable in HLM than the two 2-substituted oxetanes (compounds **20** and **21**, CL_{int,app} = 62.1 and 63.8 mL/min/kg, respectively). Examination of the metabolic profile of oxetanes **1** and **20** in NADPH-supplemented HLM (Figure 4) revealed N-dealkylation as an additional metabolic pathway (via oxidation of the bridging methylene carbon) that was not observed with 2- and 3-substituted tetrahydropyrans and tetrahydrofurans. For compound **1**, which was the most metabolically stable among all of the tested analogues, N-dealkylation was a dominant biotransformation pathway, while for compound **20**, this reaction was observed but was not the major metabolic route (see Figure 4). Compound **20** was mainly metabolized in HLM via oxetane ring scission leading to the formation of the hydroxy acid and diol metabolites (see Figure 4). Through the use of selective CYP inhibitors, it was shown that oxidative metabolism of both compounds in HLM was predominantly catalyzed by CYP3A4 because coincubation of HLM with ketoconazole, a selective CYP3A4 inhibitor, decreased metabolite formation in compounds **1** and **20** by greater than 80%. Finally, it is also worth noting that oxetanes **1**, **20**, and **21** demonstrated excellent absorptive permeability ($P_{app} > 25 \times 10^{-6}$ cm/s) in the RRCK assay, and no multidrug resistant gene (MDR1)-mediated efflux [P_{app} basolateral to apical (BA)/apical to basolateral (AB) ratio <2.0] as measured in the MDR1/Madine Darby canine kidney (MDCK) assay.¹⁴

Besides regiochemical manipulations on oxetane ring attachment, the effect of methyl substitution on the oxetane ring in 2- and 3-substituted oxetanes was also examined with respect to pharmacology and metabolism characteristics. As shown in Table 2, monomethyl substitution in 2-substituted oxetanes resulted in compounds that retained good γ -secretase potency of the nonmethylated analogues [IC₅₀ (Aβ₄₂) = 10.8 and 6.46 nM for compounds **22** and **23**, respectively] but demonstrated relatively high turnover in HLM (CL_{int,app} = 167 and 76.9 mL/min/kg). Introduction of the *gem*-dimethyl substituent adjacent to the oxetane oxygen, however, led to a 2-fold improvement in metabolic stability (compounds **2** and **3**, CL_{int,app} = 25.9 and 29.0 mL/min/kg, respectively). In addition, oxetane **2** [IC₅₀ (Aβ₄₂) = 16.5 nM] had an inhibitory potency comparable to the initial oxetane leads [compounds **20** and **1**: IC₅₀ (Aβ₄₂) = 7.99 and 16.9 nM, respectively; see Table 1]. As such, overall improvement in the disposition attributes of oxetane derivatives **1** and **2**, relative to the initial lead compound **6**, is also reflected by clear improvements in topological polar surface area (TPSA),¹⁶ lipophilic efficiency (LiPE),¹⁷ and central nervous system multiparameter optimization (CNS MPO) desirability score¹⁸ (compound **6**: TPSA = 88.9 Å², LiPE = 2.24, and CNS MPO = 3.22; compound **1**: TPSA = 98.1 Å², LiPE = 4.97, and CNS MPO = 4.71; and compound **2**: TPSA = 98.1 Å², LiPE = 3.71, and CNS MPO = 3.91). LipE and CNS MPO are key parameters to evaluate the quality and guide the selection of compounds with favorable physicochemical properties and safety profiles. As such, the clear improvement of both values suggests that the introduction of oxetanes into lead matter can

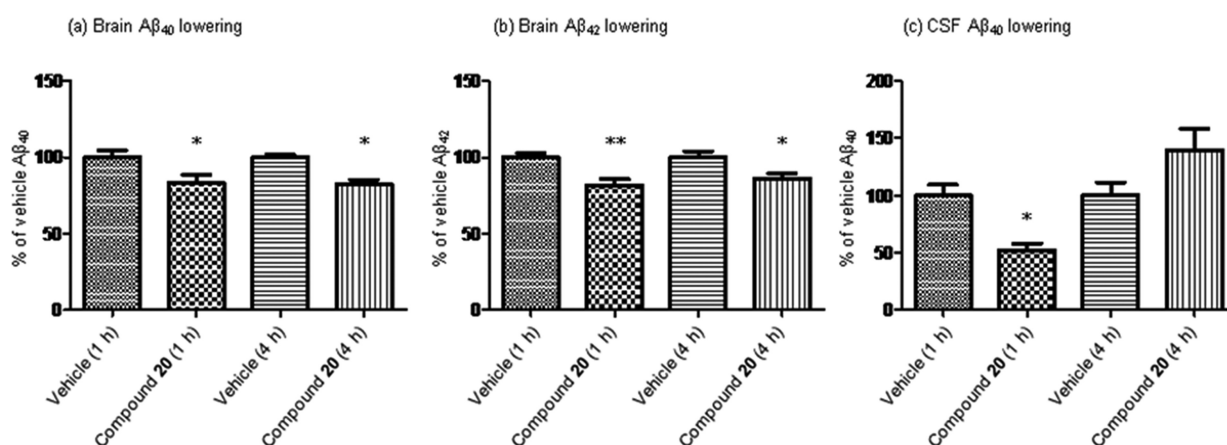


Figure 5. $A\beta$ lowering efficacy of compound **20** in brain (a and b) and CSF (c) in wild-type male 129/sve mice at 1 and 4 h after subcutaneous dosing (100 mg/kg). $A\beta$ levels were quantified by ELISA and reported as a percent of vehicle-treated mice. Data represent means \pm standard errors of the mean ($n = 5$). * $P < 0.05$ and ** $P < 0.01$ between vehicle and treated mice.

be used as a tactic to increase the overall druglikeness of molecules.

The position of the *gem*-dimethyl group on the oxetane ring appeared to be crucial for metabolic stability. For example, the two diastereomers **4** and **5** (in which the *gem*-dimethyl group occupied the C4 position on the oxetane ring) exhibited high $CL_{int,app}$ in HLM (compound **4**, $CL_{int,app} > 293$ mL/min/kg; compound **5**, $CL_{int,app} = 262$ mL/min/kg). As such, metabolite profiling of representative members of the methylated oxetanes (compounds **2**, **4**, and **5**) in HLM revealed that oxidative metabolism continued to occur on the oxetane portion of the molecules (Figure 3) implying that differences in $CL_{int,app}$ arose via individual differences in binding site affinity to the CYP enzyme(s) responsible for their metabolism.

In Vivo Pharmacology. In addition to their favorable HLM metabolic stability and in vitro γ -secretase potency described above, the oxetane derivatives also met our general criteria for Notch selectivity.^{4,5} For example, the Notch selectivity of compounds **1**, **2**, and **20** was 187-, 439-, and 523-fold (Tables 1 and 2), respectively, and was comparable to the Notch selectivity of 347-fold measured for the clinical candidate BMS-708,163. We therefore assessed whether the in vitro γ -secretase inhibitory potency of the oxetanes translated into a pharmacodynamic (PD) response in vivo. Acute γ -secretase inhibition was examined in wild-type male 129/sve mice, a validated preclinical model for evaluating pharmacokinetic (PK)/PD relationships of γ -secretase inhibitors.¹⁹ As the in vitro $CL_{int,app}$ of oxetanes **1**, **2**, and **20** in NADPH-supplemented rat liver microsomes was found to be considerably higher ($CL_{int,app} = 187$, 439, and 523 mL/min/kg, respectively) than the corresponding $CL_{int,app}$ values in HLM ($CL_{int,app} = 16.9$, 16.5, and 62.1 mL/min/kg, Tables 1 and 2), poor oral bioavailability (<5%) was discerned in both mice and rats.²⁰ Consequently, we chose the subcutaneous route of administration to bypass first pass metabolism by CYP enzymes in the mouse model. Compound **20** was used as a representative oxetane for in vivo profiling based upon its somewhat greater in vitro potency relative to **1** and **2** [compound **20**, $IC_{50}(A\beta_{42}) = 7.99$ nM, vs compounds **1** and **2**, $IC_{50}(A\beta_{42}) = 16.8$ and 16.5 nM, respectively].

Following subcutaneous administration of **20** at a dose of 100 mg/kg (chosen to ensure adequate exposure), $A\beta$ lowering was measured in brain and cerebrospinal fluid (CSF) at 1 and 4

h postdose. Corresponding exposures were also measured in these matrices to gain preliminary insight into the PK/PD relationships for γ -secretase inhibition. As shown in Figure 5, statistically significant lowering of brain $A\beta_{40}$ (at 1 h, 32%; at 4 h, 18%) and $A\beta_{42}$ (at 1 h, 19%; at 4 h, 14%) was discerned at these two time points. Although unbound brain concentrations declined sharply from 1 (1256 nM) to 4 h (141 nM) postdose, they significantly exceeded the in vitro whole cell IC_{50} value of 7.99 nM for **20**. Significant lowering of CSF $A\beta_{40}$ (48%) at 1 h postdose was also noted at a CSF concentration of 447 nM. CSF efficacy was lost at the 4 h time point (CSF concentration = 59.6 nM) with a trend toward increased $A\beta_{40}$ levels, which was not statistically significant (a scatter plot showing individual mouse CSF levels is depicted in the Supporting Information).

CONCLUSION

Via the use of in vitro metabolite identification studies, we were successful in improving the metabolic stability of the lead *N*-cyclohexylmethyl arylsulfonamide **6** in human hepatic tissue, which led to the identification of oxetane-based γ -secretase inhibitors **1** and **2**. A prominent highlight in the SAR exercise leading to oxetane-based derivatives **1** and **2** was the serendipitous discovery of the structure–metabolism differences between the 2-, 3-, and 4-substituted cycloalkyl ethers, which translated into an overall reduction in HLM clearance for the 3- and 4-substituted analogues. Metabolism differences for the 2- and 3-substituted oxetanes (compounds **1** and **20**, respectively) in HLM were rationalized in terms of differences in active site binding to CYP3A4, the principal human CYP responsible for their metabolism in liver microsomes. Whether the differences in metabolic clearance between the 2- and the 3-substituted cycloalkyl ethers observed in our studies represent a general phenomenon remains to be examined with additional examples. As such, our findings on the metabolic stability of the oxetane ring system are in good agreement with the recent reports by Carreira et al., which demonstrated the favorable disposition characteristics of oxetanes relative to certain other functional groups.⁸ Furthermore, while Carreira et al. highlighted the bioisosteric properties of oxetanes over carbonyl and *gem*-dimethyl groups, our SAR data suggest that oxetanes can offer a unique advantage over the corresponding 5- and 6-membered cycloalkanes and/or cycloalkyl ethers in terms of metabolic resistance, a finding that can be used as a general

tactic to reduce metabolic instability and improve the physicochemical properties of lead compounds. To the best of our knowledge, our metabolism studies on the oxetane ring system constitute the first report on the biotransformation of these four-membered cycloalkyl ethers. Finally, our preliminary preclinical studies with **20**, a representative member of this series, indicate that this series of γ -secretase inhibitors induces a pharmacological response in vivo by lowering $A\beta$ in both brain and CSF. Further SAR and preclinical profiling on the oxetane derivatives was suspended due to the parallel discovery of a superior chemical series. These findings will be reported in due course.

EXPERIMENTAL SECTION

Chemistry. Unless specified otherwise, starting materials were available from commercial sources. Dry solvents and reagents were of commercial quality and were used as purchased. ^1H NMR spectra were recorded on Varian INOVA spectrometers (300, 400, or 500 MHz) (Varian Inc., Palo Alto, CA) at room temperature. Chemical shifts are expressed in parts per million δ relative to residual solvent as an internal reference. Peak multiplicities are expressed as follows: singlet (s), doublet (d), triplet (t), quartet (q), multiplet (m), and broad singlet (br s). The purity of title compounds used in pharmacology testing was verified by HPLC-MS using the following method: 12 min gradient on a HP1100C pump of increasing concentrations of acetonitrile in water (5 \rightarrow 95%) containing 0.1% formic acid with a flow rate of 1 mL/min and UV detection at λ 220 and 254 nm on a Gemini C18 150 mm \times 4.6 mm, 5 μm column (Phenomenex, Torrance, CA). Title compounds used in pharmacology testing were >95% pure. Electrospray ionization mass spectra were obtained on a Waters ZQ and ZMD instrument (Milford, MA) mass spectrometer operated in positive or negative ionization mode using nitrogen as a carrier gas. All synthetic reactions were carried out under nitrogen atmosphere or in sealed vials. The chemical yields reported below are unoptimized specific examples of one preparation.

(R)-2-[4-Chloro-N-(oxetan-3-ylmethyl)phenylsulfonamido]-5,5,5-trifluoropentanamide (1). To a solution of **24** (100 mg, 0.29 mmol) and oxetan-3-ylmethanol (38.3 mg, 0.43 mmol) in tetrahydrofuran (1.5 mL) at 23 $^\circ\text{C}$ was added triphenylphosphine (115 mg, 0.43 mmol). Diethylazodicarboxylate (0.29 μL , 0.29 mmol) was then added dropwise, and the reaction mixture was stirred at that temperature for 16 h. The solvent was removed in vacuo, and the crude product was purified by preparative reverse phase HPLC [Phenomenex hydrophilic interaction liquid chromatography (HILIC, diol), 250 mm \times 21.2 mm 5 μm ; 5–100% ethanol/heptanes; flow rate = 28 mL/min] to afford 21.0 mg (17% yield) of **1** as an off-white solid. ^1H NMR (500 MHz, CDCl_3): δ 7.79–7.68 (m, 2H), 7.54 (d, J = 7.8 Hz, 2H), 6.45 (br s, 1H), 5.57 (br s, 1H), 4.71 (q, J = 6.3 Hz, 2H), 4.50 (t, J = 6.1 Hz, 1H), 4.33–4.17 (m, 2H), 3.91–3.79 (m, 1H), 3.32–3.18 (m, 2H), 2.22–2.08 (m, 1H), 2.07–1.88 (m, 1H), 1.84–1.67 (m, 1H), 1.32–1.18 (m, 1H). LC-MS (ES^+) m/z 415 ($\text{M} + \text{H}^+$); mp 142.7–144.2 $^\circ\text{C}$.

(R)-2-[4-Chloro-N-[(R)-4,4-dimethyloxetan-2-yl]methyl]phenylsulfonamido]-5,5,5-trifluoropentanamide (2) and (R)-2-[4-Chloro-N-[(S)-4,4-dimethyloxetan-2-yl]methyl]phenylsulfonamido]-5,5,5-trifluoropentanamide (3). To a suspension of **24** (150 mg, 0.43 mmol) and cesium carbonate (255 g, 0.78 mmol) in dimethylacetamide (1.0 mL) at 23 $^\circ\text{C}$ was added **26** (98.3 mg, 0.43 mmol), and the resulting reaction mixture was heated at 90 $^\circ\text{C}$ for 16 h. The reaction mixture was then cooled to 23 $^\circ\text{C}$, water (10 mL) and ethyl acetate (10 mL) were added, and the phases were separated. The aqueous phase was extracted with ethyl acetate (3 \times 10 mL), dried (MgSO_4), filtered, and concentrated in vacuo. The crude product was purified by flash column chromatography using a 0 \rightarrow 40% gradient of ethyl acetate in heptanes to give an isomeric mixture of **2** and **3**. The isomers were separated by supercritical chromatography (Chiralpak AD-H 250 mm \times 10 mm, 5 μm ; mobile phase, carbon dioxide/methanol (80/20); flow rate = 10 mL/min) to

afford 6.00 mg (3.1% yield) of **2** as a white solid and 5.00 mg (2.6% yield) of **3** as a white solid. The absolute configuration of **2** and **3** was arbitrarily assigned. Compound **2**: ^1H NMR (400 MHz, CDCl_3): δ 7.82–7.72 (m, 2H), 7.54–7.44 (m, 2H), 6.69 (br s, 1H), 5.33 (br s, 1H), 4.74 (m, 1H), 4.15 (t, J = 7.4 Hz, 1H), 3.56–3.46 (m, 1H), 3.35 (dd, J = 15.0, 9.4 Hz, 1H), 2.42 (dd, J = 11.3, 7.8 Hz, 1H), 2.22–2.08 (m, 1H), 2.04–1.91 (m, 2H), 1.90–1.68 (m, 2H), 1.41 (s, 3H), 1.34 (s, 3H). LC-MS (ES^-) m/z 441 ($\text{M} - \text{H}^-$). Compound **3**: ^1H NMR (400 MHz, CDCl_3): δ 7.81–7.74 (m, 2H), 7.52–7.46 (m, 2H), 7.37 (br s, 1H), 5.31 (br s, 1H), 4.91–4.82 (m, 1H), 4.26 (t, J = 7.5 Hz, 1H), 3.54 (dd, J = 14.4, 4.1 Hz, 1H), 3.27 (dd, J = 14.4, 9.0 Hz, 1H), 2.43 (dd, J = 11.2, 7.7 Hz, 1H), 2.34–2.22 (m, 1H), 2.21–2.06 (m, 2H), 2.03–1.85 (m, 1H), 1.65–1.55 (m, 1H), 1.39 (s, 3H), 1.34 (s, 3H). LC-MS (ES^-) m/z 441 ($\text{M} - \text{H}^-$).

(R)-2-[4-Chloro-N-[(S)-3,3-dimethyloxetan-2-yl]methyl]phenylsulfonamido]-5,5,5-trifluoropentanamide (4) and (R)-2-[4-Chloro-N-[(R)-3,3-dimethyloxetan-2-yl]methyl]phenylsulfonamido]-5,5,5-trifluoropentanamide (5). Compound **24** (289 mg, 0.84 mmol), (3,3-dimethyloxetan-2-yl)methanol (100 mg, 0.86 mmol), triphenylphosphine (336 mg, 1.26 mmol), and *t*-butyl azodicarboxylate (242 mg, 1.05 mmol) were used to synthesize **4** and **5** using the procedure described for the preparation of **1**. The crude product was purified by flash chromatography over silica using 0 \rightarrow 50% gradient of ethyl acetate in heptanes to afford 33.0 mg (8.9% yield) of **4** as a white solid and 26.0 mg (7.0% yield) of **5** as a white solid. The absolute configuration of **4** and **5** was arbitrarily assigned. Compound **4**: ^1H NMR (400 MHz, CDCl_3): δ 7.80–7.73 (m, 2H), 7.54–7.46 (m, 2H), 6.71–6.62 (m, 1H), 4.54 (dd, J = 9.7, 2.4 Hz, 1H), 4.25 (d, J = 5.7 Hz, 1H), 4.16–4.09 (m, 2H), 3.54 (dd, J = 15.2, 2.3 Hz, 1H), 3.45 (dd, J = 15.4, 9.8 Hz, 1H), 3.20–2.08 (m, 1H), 2.01–1.88 (m, 1H), 1.86–1.69 (m, 2H), 1.27 (s, 3H), 1.14 (s, 3H). LC-MS (ES^+) m/z 443 ($\text{M} + \text{H}^+$); mp 153.5–154.5 $^\circ\text{C}$. Compound **5**: ^1H NMR (400 MHz, CD_3OD): δ 7.91–7.83 (m, 2H), 7.61–7.53 (m, 2H), 4.60 (dd, J = 8.4, 3.3 Hz, 1H), 4.30 (dd, J = 8.0, 6.6 Hz, 1H), 4.22 (d, J = 5.7 Hz, 1H), 4.09 (d, J = 5.7 Hz, 1H), 3.60 (dq, J = 15.7, 5.9 Hz, 2H), 2.18–1.94 (m, 3H), 1.76–1.56 (m, 1H), 1.24 (s, 3H), 1.18 (s, 3H). LC-MS (ES^+) m/z 443 ($\text{M} + \text{H}^+$).

(R)-2-[4-Chloro-N-(cyclohexylmethyl)phenylsulfonamido]-5,5,5-trifluoropentanamide (6). Compound **24** (282 mg, 0.82 mmol), cyclohexylmethanol (112 mg, 0.98 mmol), triphenylphosphine (260 g, 0.98 mmol), and (*E*)-bis(4-chlorobenzyl)-diazene-1,2-dicarboxylate (361 mg, 0.98 mmol) were used to synthesize **6** using the procedure described for the preparation of **1**. The crude product was purified by preparative reverse phase HPLC (Phenomenex Gemini C18 column 5 μm , 150 mm \times 21.2 mm; 5–100% methanol/water with 0.1% NH_4OH ; flow rate = 28 mL/min) to afford 52.0 mg (14% yield) of **6** as an off-white solid. ^1H NMR (500 MHz, CDCl_3): δ 7.80–7.72 (m, 2H), 7.59–7.50 (m, 2H), 6.70 (br s, 1H), 5.58 (br s, 1H), 4.24 (dd, J = 9.4, 5.7 Hz, 1H), 3.21 (dd, J = 14.2, 9.8 Hz, 1H), 2.92 (dd, J = 14.2, 4.6 Hz, 1H), 2.25–2.13 (m, 1H), 2.06–1.90 (m, 1H), 1.88–1.56 (m, 7H), 1.36–1.09 (m, 4H), 1.01–0.80 (m, 2H). LC-MS (ES^+) m/z 441 ($\text{M} + \text{H}^+$); mp 170.8–171.8 $^\circ\text{C}$.

(R)-2-[4-Chloro-N-(cyclopentylmethyl)phenylsulfonamido]-5,5,5-trifluoropentanamide (7). Compound **24** (282 mg, 0.82 mmol), cyclopentylmethanol (90.1 mg, 0.90 mmol), triphenylphosphine (238 mg, 0.90 mmol), and (*E*)-bis(4-chlorobenzyl)-diazene-1,2-dicarboxylate (300 mg, 0.90 mmol) were used to synthesize **7** using the procedure described for the preparation of **1**. The crude product was purified by flash chromatography over silica using a gradient of 10 \rightarrow 40% ethyl acetate in heptanes to afford 39.0 mg (11% yield) of **7** as a white solid. ^1H NMR (500 MHz, CDCl_3): δ 7.75–7.68 (m, 2H), 7.54–7.47 (m, 2H), 6.67 (br s, 1H), 5.65 (br s, 1H), 4.20 (dd, J = 9.4, 5.7 Hz, 1H), 3.26 (dd, J = 14.1, 10.5 Hz, 1H), 2.97 (dd, J = 14.1, 5.1 Hz, 1H), 2.23–2.09 (m, 2H), 2.05–1.86 (m, 1H), 1.80–1.44 (m, 7H), 1.43–1.32 (m, 1H), 1.32–1.20 (m, 1H), 1.10–1.01 (m, 1H). LC-MS (ES^+) m/z 427 ($\text{M} + \text{H}^+$); mp 151.2–152.0 $^\circ\text{C}$.

(R)-2-[4-Chloro-N-(cyclobutylmethyl)phenylsulfonamido]-5,5,5-trifluoropentanamide (8). Compound **24** (282 mg, 0.82 mmol), cyclobutylmethanol (84.6 mg, 0.98 mmol), triphenylphosphine (238 mg, 0.90 mmol), and (*E*)-bis(4-chlorobenzyl) diazene-1,2-

dicarboxylate (361 mg, 0.98 mmol) were used to synthesize **8** using the procedure described for the preparation of **1**. The crude product was purified by preparative reverse phase HPLC (Princeton 2-ethyl pyridine 250 mm × 21.2 mm 5 μ ; 5–100% ethanol/heptanes; 28 mL/min) to afford 223 mg (66% yield) of **8** as an off-white solid. $^1\text{H NMR}$ (500 MHz, CDCl_3): δ 7.84–7.71 (m, 2H), 7.61–7.49 (m, 2H), 6.59 (br s, 1H), 5.72 (br s, 1H), 4.22 (dd, $J = 8.8, 6.1$ Hz, 1H), 3.45 (dd, $J = 14.3, 9.6$ Hz, 1H), 3.09 (dd, $J = 14.4, 5.6$ Hz, 1H), 2.63–2.51 (m, 1H), 2.24–2.13 (m, 1H), 2.09–1.92 (m, 3H), 1.92–1.68 (m, 4H), 1.66–1.56 (m, 1H), 1.40–1.23 (m, 1H). LC-MS (ES+) m/z 413 ($M + H^+$); mp 154.8–155.8 °C.

(R)-2-[4-Chloro-*N*-[(*R*)-tetrahydro-2*H*-pyran-2-yl)methyl]phenylsulfonamido]-5,5,5-trifluoropentanamide (9) and (R)-2-[4-Chloro-*N*-[(*S*)-tetrahydro-2*H*-pyran-2-yl)methyl]phenylsulfonamido]-5,5,5-trifluoropentanamide (10). To a solution of **24** (630 mg, 1.80 mmol) in dimethylformamide (3.0 mL) at 23 °C was added 2-(bromomethyl)tetrahydro-2*H*-pyran (654 mg, 3.60 mmol) followed by cesium carbonate (1.19 g, 3.60 mmol). The reaction mixture was heated at 80 °C for 16 h, then cooled to 23 °C, and filtered through Celite. The resulting filtrate was concentrated in vacuo, and the crude product was purified by flash chromatography over silica using a 30 → 50% gradient of ethyl acetate in heptanes to afford 89.0 mg (11% yield) of **9** as a white solid and 36.0 mg (4.5% yield) of **10** as a white solid. The absolute configuration of **9** and **10** was arbitrarily assigned. Compound **9**: $^1\text{H NMR}$ (400 MHz, CD_3OD): δ 7.91–7.87 (m, 2H), 7.63–7.59 (m, 2H), 4.40 (dd, $J = 8.5, 6.4$ Hz, 1H), 3.79 (dd, $J = 10.7, 2.1$ Hz, 1H), 3.64–3.56 (m, 1H), 3.42 (dd, $J = 15.0, 3.0$ Hz, 1H), 3.25–3.14 (m, 2H), 2.27–2.08 (m, 3H), 2.07–1.95 (m, 1H), 1.86–1.73 (m, 2H), 1.61 (d, $J = 12.7$ Hz, 1H), 1.54–1.46 (m, 2H), 1.24–1.16 (m, 1H). LC-MS (ES+) m/z 443 ($M + H^+$). Compound **10**: $^1\text{H NMR}$ (400 MHz, CD_3OD): δ 7.86–7.82 (m, 2H), 7.60–7.56 (m, 2H), 4.36–4.32 (m, 1H), 3.87 (dd, $J = 11.6, 2.8$ Hz, 1H), 3.61 (ddt, $J = 11.1, 8.6, 2.4$ Hz, 1H), 3.41–3.33 (m, 3H), 2.39–2.31 (m, 1H), 2.05–1.91 (m, 3H), 1.89–1.83 (m, 1H), 1.65–1.58 (m, 1H), 1.57–1.48 (m, 3H), 1.15 (dd, $J = 11.4, 4.3$ Hz, 1H). LC-MS (ES+) m/z 443 ($M + H^+$); mp 187.8–188.7 °C.

(R)-2-[4-Chloro-*N*-[(*R*)-tetrahydro-2*H*-pyran-3-yl)methyl]phenylsulfonamido]-5,5,5-trifluoropentanamide (11) and (R)-2-[4-Chloro-*N*-[(*S*)-tetrahydro-2*H*-pyran-3-yl)methyl]phenylsulfonamido]-5,5,5-trifluoropentanamide (12). To a solution of (tetrahydro-2*H*-pyran-3-yl)methanol (505 mg, 4.35 mmol) and triethylamine (660 mg, 6.52 mmol) in dichloromethane (10 mL) at 0 °C was added methane sulfonyl chloride (598 mg, 5.22 mmol), and the reaction mixture was stirred at that temperature for 0.5 h. A 1 M aqueous solution of hydrochloric acid (10 mL) was then added, the phases were separated, and the organic phase was extracted with dichloromethane (2 × 10 mL). The combined organic phases were washed with a saturated aqueous solution of sodium bicarbonate (10 mL) and brine (10 mL). The organic phase was dried (MgSO_4), filtered, and concentrated in vacuo to give a clear oil. To a solution of this crude product in dimethylformamide (3.0 mL) at 23 °C was added **24** (500 mg, 1.45 mmol) followed by cesium carbonate (945 mg, 2.90 mmol). The resulting reaction mixture was heated at 80 °C for 16 h. The reaction mixture was then cooled to 23 °C and filtered over Celite, and the resulting filtrate was concentrated in vacuo. The crude product was purified by flash chromatography over silica using a 0 → 2.5% gradient of methanol in dichloromethane to give an isomeric mixture of **11** and **12** as a white solid. The isomers were separated by supercritical chromatography (Chiralpak AD-H 250 mm × 10 mm; 20% methanol/carbon dioxide; 10 mL/min) to afford 36.0 mg (5.6% yield) of **11** white solid and 35.0 mg (5.5% yield) of **12** as a white solid. The absolute configuration of **11** and **12** was arbitrarily assigned. Compound **11**: $^1\text{H NMR}$ (400 MHz, $\text{DMSO}-d_6$): δ 7.90–7.86 (m, 2H), 7.70–7.66 (m, 2H), 7.32 (br s, 1H), 7.24 (br s, 1H), 4.30 (dd, $J = 7.5, 7.5$ Hz, 1H), 3.77 (dd, $J = 10.9, 2.5$ Hz, 1H), 3.72–3.66 (m, 1H), 3.31–3.23 (m, 2H), 3.07–2.93 (m, 2H), 2.16–2.05 (m, 2H), 2.02–1.93 (m, 1H), 1.58–1.51 (m, 1H), 1.49–1.32 (m, 3H), 1.21–1.11 (m, 2H). LC-MS (ES+) m/z 443 ($M + H^+$). Compound **12**: $^1\text{H NMR}$ (400 MHz, $\text{DMSO}-d_6$): δ 7.89–7.85 (m, 2H), 7.69–7.65 (m, 2H), 7.30 (br s, 1H), 7.24 (br s, 1H), 4.29 (dd, $J = 7.4, 7.4$ Hz, 1H), 3.79–

3.68 (m, 1H), 3.28–3.20 (m, 1H), 3.05–2.97 (m, 2H), 2.19–2.09 (m, 2H), 2.02–1.93 (m, 2H), 1.89–1.80 (m, 1H), 1.74 (d, $J = 9.6$ Hz, 1H), 1.59–1.35 (m, 3H), 1.18–1.07 (m, 2H). LC-MS (ES+) m/z 443 ($M + H^+$); mp 126.0–127.0 °C.

(R)-2-[4-Chloro-*N*-[(tetrahydro-2*H*-pyran-4-yl)methyl]phenylsulfonamido]-5,5,5-trifluoropentanamide (13). To a solution of **24** (300 mg, 0.87 mmol) and 4-(iodomethyl)tetrahydro-2*H*-pyran (295 mg, 1.30 mmol) in dimethylformamide (4.4 mL) at 23 °C was added cesium carbonate (510 mg, 1.57 mmol). The reaction mixture was then heated at 80 °C for 16 h. Ethyl acetate (20 mL) and water (10 mL) were then added, the phases were separated, and the organic phase was washed with a saturated aqueous solution of sodium bicarbonate (10 mL), water (10 mL), and brine (10 mL). The organic phase was dried (Na_2SO_4), filtered, and concentrated in vacuo. The crude product was purified by flash chromatography over silica using a 10 → 100% gradient of ethyl acetate in heptanes to afford 223 mg (58% yield) of **13** as a white solid. $^1\text{H NMR}$ (400 MHz, CDCl_3): δ 7.74–7.69 (m, 2H), 7.53–7.49 (m, 2H), 6.63 (br s, 1H), 5.44 (br s, 1H), 4.21 (dd, $J = 9.5, 5.6$ Hz, 1H), 3.98–3.88 (m, 2H), 3.38–3.19 (m, 3H), 2.91 (dd, $J = 14.4, 4.8$ Hz, 1H), 2.21–2.09 (m, 1H), 2.02–1.80 (m, 2H), 1.78–1.64 (m, 2H), 1.47 (d, $J = 13.1$ Hz, 1H), 1.37–1.13 (m, 3H). LC-MS (ES-) m/z 441 ($M - H^-$).

(R)-2-[*N*-[(*R*)-1,4-Dioxan-2-yl)methyl]-4-chlorophenylsulfonamido]-5,5,5-trifluoropentanamide (14). (*R*)-1,4-Dioxan-2-yl)methanol (257 mg, 2.18 mmol), triethylamine (330 mg, 3.26 mmol), methane sulfonyl chloride (299 mg, 2.61 mmol), compound **24** (250 mg, 0.72 mmol), and cesium carbonate (472 mg, 1.45 mmol) were used to synthesize **14** using the procedure described for the preparation of **11** and **12**. The crude product was purified by flash chromatography over silica using a 0 → 5% gradient of methanol in dichloromethane to afford 39.0 mg (12% yield) of **14** as a white solid. $^1\text{H NMR}$ (400 MHz, CDCl_3): δ 7.80–7.75 (m, 2H), 7.54–7.49 (m, 2H), 7.00 (br s, 1H), 5.38 (br s, 1H), 4.35 (t, $J = 7.5$ Hz, 1H), 3.89–3.81 (m, 1H), 3.78 (dd, $J = 11.4, 2.5$ Hz, 1H), 3.69–3.61 (m, 2H), 3.54 (dt, $J = 11.1, 2.1$ Hz, 1H), 3.48–3.41 (m, 1H), 3.34–3.20 (m, 2H), 3.09 (dd, $J = 14.8, 8.7$ Hz, 1H), 2.35–2.24 (m, 1H), 2.15–2.03 (m, 1H), 1.89 (dtd, $J = 15.4, 10.3, 5.2$ Hz, 1H), 1.54–1.48 (m, 1H). LC-MS (ES+) m/z 445 ($M + H^+$).

(R)-2-[*N*-[(*S*)-1,4-Dioxan-2-yl)methyl]-4-chlorophenylsulfonamido]-5,5,5-trifluoropentanamide (15). (*S*)-1,4-Dioxan-2-yl)methanol (257 mg, 2.18 mmol), triethylamine (330 mg, 3.26 mmol), methane sulfonyl chloride (299 mg, 2.61 mmol), compound **24** (250 mg, 0.72 mmol), and cesium carbonate (472 mg, 1.45 mmol) were used to synthesize **15** using the procedure described for the preparation of **11** and **12**. The crude product was purified by flash chromatography over silica using a 0 → 5% gradient of methanol in dichloromethane to afford 86.0 mg (27% yield) of **15** as a white solid. $^1\text{H NMR}$ (400 MHz, CDCl_3): δ 7.77–7.73 (m, 2H), 7.53–7.48 (m, 2H), 6.55 (br s, 1H), 5.41 (br s, 1H), 4.18 (dd, $J = 8.4, 6.1$ Hz, 1H), 3.82 (tt, $J = 9.4, 2.7$ Hz, 1H), 3.74–3.68 (m, 2H), 3.68–3.64 (m, 1H), 3.56–3.51 (m, 2H), 3.24–3.21 (m, 1H), 3.20–3.11 (m, 2H), 2.13–2.03 (m, 1H), 1.97–1.66 (m, 3H). LC-MS (ES+) m/z 445 ($M + H^+$).

(R)-2-[4-Chloro-*N*-[(*R*)-tetrahydrofuran-3-yl)methyl]phenylsulfonamido]-5,5,5-trifluoropentanamide (16) and (R)-2-[4-Chloro-*N*-[(*S*)-tetrahydrofuran-3-yl)methyl]phenylsulfonamido]-5,5,5-trifluoropentanamide (17). Compound **24** (345 mg, 1.00 mmol), (tetrahydrofuran-3-yl)methanol (128 mg, 1.25 mmol), triphenylphosphine (333 mg, 1.25 mmol), and diethyl azodicarboxylate (0.20 mL, 1.25 mmol) were used to synthesize **16** and **17** using the procedure described for the preparation of **1**. The crude product was purified by flash chromatography over silica using a 20 → 100% gradient of ethyl acetate in heptanes to give an isomeric mixture of **16** and **17**. The isomers were separated by supercritical fluid chiral chromatography (10 mm × 250 mm Chiralpak AD-H column; 80/20 CO_2 /methanol isocratic gradient over 7.5 min; flow rate = 10 mL/min) to afford 34.0 mg (7.9% yield) of **16** as a white foam and 30.0 mg (7.0% yield) of **17** as a white foam. The absolute configuration of **17** was determined using X-ray crystallography. Compound **16**: $^1\text{H NMR}$ (500 MHz, CDCl_3): δ 7.81–7.70 (m, 2H), 7.62–7.48 (m, 2H), 6.69 (br s, 1H),

5.50 (br s, 1H), 4.29 (dd, $J = 9.6, 5.3$ Hz, 1H), 4.04–3.86 (m, 1H), 3.83–3.68 (m, 2H), 3.56–3.35 (m, 2H), 3.00 (dd, $J = 14.4, 4.9$ Hz, 1H), 2.66–2.49 (m, 1H), 2.30–2.13 (m, 1H), 2.08–1.85 (m, 3H), 1.85–1.64 (m, 1H), 1.34–1.18 (m, 1H). LC-MS (ES+) m/z 429 ($M + H^+$). Compound 17: 1H NMR (500 MHz, $CDCl_3$): δ 7.79–7.72 (m, 2H), 7.59–7.52 (m, 2H), 6.62 (br s, 1H), 5.47 (br s, 1H), 4.27 (dd, $J = 9.8, 5.4$ Hz, 1H), 3.90 (dt, $J = 8.4, 5.0$ Hz, 1H), 3.77–3.68 (m, 3H), 3.44 (dd, $J = 14.3, 10.6$ Hz, 1H), 3.05 (dd, $J = 14.5, 5.0$ Hz, 1H), 2.63–2.54 (m, 1H), 2.26–2.17 (m, 1H), 2.07–1.97 (m, 2H), 1.84–1.71 (m, 1H), 1.52–1.44 (m, 1H), 1.29 (dt, $J = 14.5, 5.9$ Hz, 1H). LC-MS (ES+) m/z 429 ($M + H^+$); mp 151.3–153.2 °C.

(*R*)-2-{4-Chloro-*N*-[(*R*)-tetrahydrofuran-2-yl]methyl]phenylsulfonamido}-5,5,5-trifluoropentanamide (18) and (*R*)-2-{4-Chloro-*N*-[(*S*)-tetrahydrofuran-2-yl]methyl]phenylsulfonamido}-5,5,5-trifluoropentanamide (19). Compound 24 (500 mg, 1.45 mmol), (tetrahydrofuran-2-yl)methanol (141 μ L, 1.45 mmol), triphenylphosphine (579 mg, 2.18 mmol), and diethyl azodicarboxylate (286 μ L, 1.45 mmol) were used to synthesize 18 and 19 using the procedure described for the preparation of 1. The crude product was purified by preparative reverse phase HPLC (Phenomenex Kinetex C18 column, 50 mm \times 3.0 mm 2.6 μ ; 0–100% methanol/water with 0.1% formic acid; flow rate = 1.0 mL/min) to afford 110 mg (18% yield) of 18 as a white solid and 15 mg (2.4% yield) of 19 as a white solid. The absolute configuration of 18 and 19 was arbitrarily assigned. Compound 18: 1H NMR (500 MHz, $CDCl_3$): δ 7.82 (d, $J = 8.4$ Hz, 2H), 7.52 (d, $J = 8.4$ Hz, 2H), 6.98 (s, 1H), 5.66 (s, 1H), 4.22–4.13 (m, 2H), 3.84–3.71 (m, 2H), 3.42 (dd, $J = 15.0, 2.3$ Hz, 1H), 3.13 (dd, $J = 15.0, 10.0$ Hz, 1H), 2.22–2.14 (m, 1H), 2.07–1.72 (m, 6H), 1.49–1.41 (m, 1H). LC-MS (ES+) m/z 429 ($M + H^+$); mp 150.0–151.0 °C. Compound 19: 1H NMR (500 MHz, $CDCl_3$): δ 7.85–7.82 (m, 2H), 7.53–7.50 (m, 2H), 7.46 (s, 1H), 5.48 (s, 1H), 4.35–4.25 (m, 2H), 3.81–3.67 (m, 2H), 3.41 (dd, $J = 14.6, 3.5$ Hz, 1H), 3.09 (dd, $J = 14.6, 9.6$ Hz, 1H), 2.37–2.27 (m, 1H), 2.24–1.88 (m, 6H), 1.57–1.48 (m, 1H). LC-MS (ES+) m/z 429 ($M + H^+$).

(*R*)-2-{4-Chloro-*N*-[(*S*)-oxetan-2-yl]methyl]phenylsulfonamido}-5,5,5-trifluoropentanamide (20) and (*R*)-2-{4-Chloro-*N*-[(*R*)-oxetan-2-yl]methyl]phenylsulfonamido}-5,5,5-trifluoropentanamide (21). Compound 24 (3.14 g, 9.10 mmol), oxetan-2-ylmethanol (960 mg, 10.9 mmol), triphenylphosphine (3.61 g, 13.6 mmol), and diethyl azodicarboxylate (2.31 mL, 13.6 mmol) were used to synthesize 20 and 21 using the procedure described for the preparation of 1. The crude product was purified by preparative reverse phase HPLC (Phenomenex Amylose-2 250 mm \times 21.2 mm, 5 μ ; 5–100% ethanol/heptanes; flow rate = 28 mL/min) to afford 698 mg (19% yield) of 20 as an off-white solid and 425 mg (11% yield) of 21 as an off-white solid. The absolute configuration of 20 and 21 was determined using X-ray crystallography. Compound 20: 1H NMR (500 MHz, $CDCl_3$): δ 7.82–7.70 (m, 2H), 7.58–7.41 (m, 2H), 6.63 (br s, 1H), 5.45 (br s, 1H), 5.03–4.94 (m, 1H), 4.61 (ddd, $J = 8.5, 7.3, 6.1$ Hz, 1H), 4.47 (dt, $J = 9.1, 6.1$ Hz, 1H), 4.14 (t, $J = 7.4$ Hz, 1H), 3.52–3.49 (m, 2H), 2.75–2.64 (m, 1H), 2.33–2.21 (m, 1H), 2.19–2.08 (m, 1H), 2.01–1.65 (m, 3H). LC-MS (ES+) m/z 415 ($M + H^+$); mp 134.8–137.6 °C. Compound 21: 1H NMR (500 MHz, $CDCl_3$): δ 7.84–7.71 (m, 2H), 7.54–7.45 (m, 2H), 7.22–7.11 (m, 1H), 5.34 (br s, 1H), 5.13–4.99 (m, 1H), 4.66–4.59 (m, 1H), 4.51 (dt, $J = 9.2, 6.2$ Hz, 1H), 4.27 (t, $J = 7.5$ Hz, 1H), 3.56–3.43 (m, 2H), 2.78–2.68 (m, 1H), 2.38–2.22 (m, 2H), 2.21–2.03 (m, 1H), 2.01–1.82 (m, 1H), 1.63–1.50 (m, 1H). LC-MS (ES+) m/z 415 ($M + H^+$); mp 146.6–148.9 °C.

(*R*)-2-{4-Chloro-*N*-[(2*S*,4*S*)-4-methyloxetan-2-yl]methyl]phenylsulfonamido}-5,5,5-trifluoropentanamide (22) and (*R*)-2-{4-Chloro-*N*-[(2*S*,4*R*)-4-methyloxetan-2-yl]methyl]phenylsulfonamido}-5,5,5-trifluoropentanamide (23). To a solution of 24 (580 mg, 1.68 mmol) in dimethylacetamide (1.0 mL) at 23 °C was added cesium carbonate (1.10 g, 3.36 mmol), and the resulting mixture was heated at 60 °C for 15 min. Compound 25 (357 mg, 1.68 mmol) was then added, and the resulting mixture was heated at this temperature for 16 h. The reaction mixture was then cooled to 23 °C, water (20 mL) and ethyl acetate (20 mL) were added, and the phases were separated. The aqueous phase was extracted with ethyl

acetate (2 \times 20 mL), and the combined organic phases were dried ($MgSO_4$), filtered, and concentrated in vacuo. The crude product was purified by chiral HPLC [Chiralpak AD-H 250 mm \times 10 mm, 5 μ ; mobile phase, carbon dioxide/methanol (80/20), 10 mL/min] to afford 6.00 mg (0.8% yield) of 22 as a white solid and 14.0 mg (1.9% yield) of 23 as a white solid. The relative configuration of 22 and 23 was assigned using a set of two-dimensional NMR spectroscopy experiments (COSY and NOE), and the absolute configuration was arbitrarily assigned. Compound 22: 1H NMR (400 MHz, $CDCl_3$): δ 7.81–7.73 (m, 2H), 7.55–7.45 (m, 2H), 6.66 (br s, 1H), 5.43 (br s, 1H), 4.90–4.76 (m, 2H), 4.19–4.10 (m, 1H), 3.52 (dd, $J = 15.2, 2.9$ Hz, 1H), 3.33 (dd, $J = 15.1, 9.5$ Hz, 1H), 2.73 (dt, $J = 11.3, 7.2$ Hz, 1H), 2.21–2.07 (m, 1H), 2.05–1.90 (m, 1H), 1.88–1.69 (m, 3H), 1.32 (d, $J = 6.1$ Hz, 3H). LC-MS (ES-) m/z 427 ($M - H^-$); mp 107.0–109.0 °C. Compound 23: 1H NMR (400 MHz, $CDCl_3$): δ 7.83–7.68 (m, 2H), 7.56–7.44 (m, 2H), 6.68 (br s, 1H), 5.42 (br s, 1H), 4.88–4.70 (m, 2H), 4.14 (t, $J = 7.4$ Hz, 1H), 3.54–3.48 (m, 2H), 2.40–2.23 (m, 2H), 2.22–2.08 (m, 1H), 2.04–1.87 (m, 1H), 1.88–1.65 (m, 2H), 1.39 (d, $J = 6.2$ Hz, 3H). LC-MS (ES-) m/z 427 ($M - H^-$).

2-(Iodomethyl)-4-methyloxetane (25). To a slurry of *bis*(*sym*-collidine)silver(I) perchlorate (7.55 g, 16.3 mmol) in dichloromethane (75 mL) at 23 °C was added iodine (4.21 g, 16.3 mmol) in one portion, and the resulting mixture was stirred at that temperature for 20 min (during which time AgI precipitated from the reaction mixture). 2-Methylpent-4-en-2-ol (1.00 g, 11.6 mmol) was then added in one portion at that temperature, and the reaction mixture was stirred for 16 h. The reaction mixture was then filtered through Celite, and the crude product was washed with dichloromethane (20 mL). The resulting filtrate was washed with a 10% aqueous solution of sodium sulfite (2 \times 30 mL), a 10% aqueous solution of hydrochloric acid (2 \times 50 mL), dried (K_2CO_3), filtered, and concentrated in vacuo. The crude product was used in the next step without purification.

4-(Iodomethyl)-2,2-dimethyloxetane (26). *bis*(*sym*-Collidine)-silver(I) perchlorate (6.50 g, 14.0 mmol), iodine (3.63 g, 14.0 mmol), and 2-methylpent-4-en-2-ol (1.00 g, 10.0 mmol) were used to synthesize 26 using the procedure described for the preparation of 25. The crude product was used in the next step without purification.

(3,3-Dimethyloxetan-2-yl)methanol (30). To a solution of methyl 3,3-dimethyloxetan-2-carboxylate (2.90 g, 20.1 mmol) in tetrahydrofuran (58 mL) was added lithium aluminum hydride (783 mg, 20.6 mmol) at –30 °C, and the resulting mixture was stirred at this temperature for 1.5 h. Water (50 mL) and dichloromethane (100 mL) were then added, the phases were separated, and the aqueous phase was extracted with dichloromethane (2 \times 100 mL). The combined organic phases were dried (Na_2SO_4), filtered, and concentrated in vacuo to afford 1.20 g (51% yield) of 30 as a yellow oil. 1H NMR (400 MHz, $CDCl_3$): δ 4.38 (s, 1H), 4.26 (d, $J = 5.6$ Hz, 1H), 4.21 (d, $J = 5.6$ Hz, 1H), 3.83–3.78 (m, 1H), 3.69–3.65 (m, 1H), 1.26 (s, 3H), 1.14 (s, 3H). LC-MS (ES-) m/z 99.1 ($M - 17$, loss of OH).

In Vitro Metabolism Studies. Test compounds (10 μ M) were incubated with pooled HLM (1.0 mg/mL; BD Gentest, Woburn, MA) in 1 mL of potassium phosphate (100 mM, pH 7.4) containing $MgCl_2$ (3.3 mM) and NADPH (1.3 mM). Incubations were carried out in a shaking water bath set at 37 °C open to air. At 5 and 30 min, 0.5 mL of the incubation mixture was added to 5 mL of acetonitrile to terminate the reactions. The mixtures were centrifuged (1700g) for 5 min, and the supernatants were evaporated in a vacuum centrifuge. The residues were reconstituted in 0.2 mL of 0.1% formic acid in water and injected (0.06 mL) onto an HPLC system. The HPLC system consisted of a ThermoFinnigan Surveyor system interfaced with a ThermoFinnigan LTQ mass spectrometer. Separation was effected on a Varian Polaris C18 column (4.6 mm \times 250 mm; 5 μ particle size) equilibrated in 0.1% formic acid in 10% acetonitrile at a flow rate of 0.8 mL/min. This mobile phase composition was maintained for 5 min followed by a linear gradient of increasing acetonitrile to 90% at 50 min. This was followed by a 10 min of reequilibration at initial conditions. The eluent was passed through a photodiode array UV detector followed by introduction of a split of \sim 50 μ L/min into the mass spectrometer.

Analysis was done in both positive and negative ion mode in separate injections. Tune file settings in each mode were optimized for the signal for compound **6**. MS² and MS³ data were gathered with data-dependent scanning of the three most intense ions. To verify the identity of metabolites, samples were also analyzed on a ThermoFinnigan Orbitrap mass spectrometer operated at a resolution setting of 30000 to gather high-resolution mass spectral data. HPLC conditions used were the same as above. The metabolism of compounds **1** and **20** was also examined in the presence of CYP-specific inhibitors. Incubations were carried out as above, in the presence and absence of furafylline (20 μ M), sulfaphenazole (5 μ M), *N*-benzylrivanol (20 μ M), quinidine (1 μ M), or ketoconazole (1 μ M), except that incubations were carried out for 40 min. Samples were processed as above and analyzed by HPLC-MS for metabolite formation.

■ ASSOCIATED CONTENT

● Supporting Information

X-ray crystallography data for compounds **17** and **20**, mass spectral fragmentation data for compounds **1** and **20**, ¹H NMR spectra of compounds **1**, **2**, and **6**, experimental details for in vivo pharmacology, and scatter plots for Figure 5. This material is available free of charge via the Internet at <http://pubs.acs.org>.

■ AUTHOR INFORMATION

Corresponding Author

*Tel: 860-686 3247. E-mail: Antonia.Stepan@pfizer.com.

■ ACKNOWLEDGMENTS

We thank Drs. Amit S. Kalgutkar, Robert Dow, and Patrick R. Verhoest for helpful suggestions in preparing this article and Brian Samas and Ivan Samardjiev for the single crystal X-ray structure elucidation of compounds **17** and **20**. We also thank James Bradow, Robert P. Depianta, and Drs. Qi Yan and Laurence Philippe-Venec from the purification group and Brendon Kapinos, Walter E. Mitchell, Jillian B. Van Hausen, James J. Frederico, III, John P. Umland, Mark W. Snyder, and Dr. Marina Y. Shalaeva from the ADME high-throughput screening group at Pfizer, Groton.

■ ABBREVIATIONS USED

A β , amyloid- β peptide; AD, Alzheimer's disease; BA, basolateral to apical; CL_{int,app}, apparent intrinsic clearance; CNS MPO, central nervous system multiparameter optimization; CSF, cerebrospinal fluid; CYP, cytochrome P450; HLM, human liver microsomes; LiPE, lipophilic efficiency; MDCK, Madine Darby canine kidney; MDR1, multidrug resistance protein (*p*-glycoprotein); PK, pharmacokinetic; PD, pharmacodynamic; SAR, structure–activity relationship; TPSA, topological polar surface area

■ REFERENCES

- (1) Ferri, C.; Prince, M.; Brayne, C.; Brodaty, H.; Fratiglioni, L.; Ganguli, M.; Hall, K.; Hasegawa, K.; Hendrie, H.; Huang, Y. Global prevalence of dementia: A Delphi consensus study. *Lancet* **2005**, *366*, 2112–2117.
- (2) Hardy, J.; Selkoe, D. J. The amyloid hypothesis of Alzheimer's disease: progress and problems on the road to therapeutics. *Science* **2002**, *297*, 353–356.
- (3) (a) Sinha, S.; Liberburg, I. Cellular mechanisms of β -amyloid production and secretion. *Proc. Natl. Acad. Sci. U.S.A.* **1999**, *96*, 11049–11053. (b) Bergmans, B. A.; De Strooper, B. γ -secretases: From cell biology to therapeutic strategies. *Lancet Neurol.* **2010**, *9*, 215–226. (c) Wolfe, M. S. The γ -secretase complex: Membrane-embedded proteolytic ensemble. *Biochemistry* **2006**, *45*, 7931–7939.

(4) Kopan, R.; Ilagan, M. X. γ -Secretase: Proteasome of the membrane? *Nat. Rev. Mol. Cell. Biol.* **2004**, *5*, 499–504.

(5) (a) Wong, G. T.; Manfra, D.; Poulet, F. M.; Zhang, Qi; Josien, H.; Bara, T.; Engstrom, L.; Pinzon-Ortiz, M.; Fine, J. S.; Lee, H.-J. J.; Zhang, L.; Higgins, G. A.; Parker, E. M. Chronic treatment with the γ -secretase inhibitor LY-411,575 inhibits β -amyloid peptide production and alters lymphopoiesis and intestinal cell differentiation. *J. Biol. Chem.* **2004**, *279*, 12876–12882. (b) Barten, D. M.; Meredith, J. E. Jr.; Zaczek, R.; Houston, J. G.; Albright, C. F. Gamma-secretase inhibitors for Alzheimer's disease: Balancing efficacy and toxicity. *Drugs R. D.* **2006**, *7*, 87–97.

(6) For a review, see Kreft, A. F.; Martone, R.; Porte, A. Recent advances in the identification of γ -secretase inhibitors to clinically test the A β oligomer hypothesis of Alzheimer's disease. *J. Med. Chem.* **2009**, *52*, 6169–6188. For examples, see: (a) Sparey, T.; Behr, D.; Best, J.; Biba, M.; Castro, J. L.; Clarke, E.; Hannam, J.; Harrison, T.; Lewis, H.; Madin, A.; Shearman, M.; Sohal, B.; Tsou, N.; Welch, C.; Wrigley, J. Cyclic sulfamide γ -secretase inhibitors. *Bioorg. Med. Chem. Lett.* **2005**, *15*, 4212–4216. (b) Kitas, E. A.; Galley, G.; Jakob-Roetne, R.; Flohr, A.; Wostl, W.; Mauser, H.; Alker, A. M.; Czech, C.; Ozmen, L.; David-Pierson, P.; Reinhardt, D.; Jacobsen, H. Substituted 2-oxoazepane derivatives are potent, orally active γ -secretase inhibitors. *Bioorg. Med. Chem. Lett.* **2008**, *18*, 304–308. (c) Prasad, C. V. C.; Zheng, M.; Vig, S.; Bergstrom, C.; Smith, D. W.; Gao, Q.; Yeola, S.; Polson, C. T.; Corsa, J. A.; Guss, V. L.; Loo, A.; Wang, J.; Slecza, B. G.; Dangler, C.; Robertson, B. J.; Hendrick, J. P.; Roberts, S. B.; Barten, D. M. Discovery of (S)-2-((S)-2-(3,5-difluorophenyl)-2-hydroxyacetamido)-N-((S,Z)-3-methyl-4-oxo-4,5-dihydro-3H-benzodiazepin-5-yl)propanamide (BMS-433796): A γ -secretase inhibitor with A β lowering activity in a transgenic mouse model of Alzheimer's disease. *Bioorg. Med. Chem. Lett.* **2007**, *17*, 4006–4011. (d) Pissarnitski, D. A.; Asberom, T.; Bara, T. A.; Buevich, A. V.; Clader, J. W.; Greenlee, W. J.; Guzik, H. S.; Josien, H. B.; Li, W.; McEwan, M.; McKittrick, B. A.; Nechuta, T. L.; Parker, E. M.; Sinning, L.; Smith, E. M.; Song, L.; Vaccaro, H. A.; Voigt, J. H.; Zhang, L.; Zhang, Q.; Zhao, Z. 2,6-Disubstituted N-arylsulfonyl piperidines as γ -secretase inhibitors. *Bioorg. Med. Chem. Lett.* **2007**, *17*, 57–62. (e) Jelley, R. A.; Elliott, J.; Gibson, K. R.; Harrison, T.; Behr, D.; Clarke, E. E.; Lewis, H. D.; Shearman, M.; Wrigley, J. D. J. 3-Substituted gem-cyclohexane sulfone based γ -secretase inhibitors for Alzheimer's disease: Conformational analysis and biological activity. *Bioorg. Med. Chem. Lett.* **2006**, *16*, 3839–3842. (f) Fuwa, H.; Hiromoto, K.; Takahashi, Y.; Yokoshima, S.; Kan, T.; Fukuyama, T.; Iwatsubo, T.; Tomita, T.; Natsugari, H. Synthesis of biotinylated photoaffinity probes based on arylsulfonamide γ -secretase inhibitors. *Bioorg. Med. Chem. Lett.* **2006**, *16*, 4184–4189. (g) Asberom, T.; Zhao, Z.; Bara, T. A.; Clader, J. W.; Greenlee, W. J.; Hyde, L. A.; Josien, H. B.; Li, W.; McPhail, A. T.; Nomeir, A. A.; Parker, E. M.; Rajagopalan, M.; Song, L.; Wong, G. T.; Zhang, L.; Zhang, Q.; Pissarnitski, D. A. Discovery of γ -secretase inhibitors efficacious in a transgenic animal model of Alzheimer's disease. *Bioorg. Med. Chem. Lett.* **2007**, *17*, 511–516. (h) Guo, T.; Gu, H.; Hobbs, D. W.; Rokosz, L. L.; Stauffer, T. M.; Jacob, B.; Clader, J. W. Design, synthesis, and evaluation of tetrahydroquinoline and pyrrolidine sulfonamide carbamates as γ -secretase inhibitors. *Bioorg. Med. Chem. Lett.* **2007**, *17*, 3010–3013. (i) Lewis, S. J.; Gu, H.; Hobbs, D. W.; Rokosz, L. L.; Stauffer, T. M.; Jacob, B.; Clader, J. W. A novel series of potent γ -secretase inhibitors based on a benzobicyclo[4.2.1]nonane core. *Bioorg. Med. Chem. Lett.* **2005**, *15*, 373–378. (j) Truong, A. P.; Aubele, D. A.; Probst, G. D.; Neitzel, M. L.; Semko, C. M.; Bowers, S.; Dressen, D.; Hom, R. K.; Konradi, A. W.; Sham, H. L.; Garofalo, A. W.; Keim, P. S.; Wu, J.; Dappen, M. S.; Wong, K.; Goldbach, E.; Quinn, K. P.; Sauer, J.-M.; Brigham, E. F.; Wallace, W.; Nguyen, L.; Hemphill, S. S.; Bova, M. P.; Basi, G. Design, synthesis, and structure-activity relationship of novel orally efficacious pyrazole/sulfonamide based dihydroquinoline γ -secretase inhibitors. *Bioorg. Med. Chem. Lett.* **2009**, *19*, 4920–4923. (k) Brodney, M. A.; Auperin, D. D.; Becker, S. L.; Bronk, B. S.; Brown, T. M.; Coffman, K. J.; Finley, J. E.; Hicks, C. D.; Karmilowicz, M. J.; Lanz, T. A.; Liston, D.; Liu, X.; Martin, B.-A.; Nelson, R. B.; Nolan, C.

- E.; Oborski, C. E.; Parker, C. P.; Richter, K. E. G.; Pozdnyakov, N.; Sahagan, B. G.; Schachter, J. B.; Sokolowski, S. A.; Tate, B.; Van Deusen, J. W.; Wood, D. E.; Wood, K. M. Diamide amino-imidazoles: A novel series of γ -secretase inhibitors for the treatment of Alzheimer's disease. *Bioorg. Med. Chem. Lett.* **2011**, *21*, 2631–2636. (1) Brodney, M. A.; Auperin, D. D.; Becker, S. L.; Bronk, B. S.; Brown, T. M.; Coffman, K. J.; Finley, J. E.; Hicks, C. D.; Karmilowicz, M. J.; Lanz, T. A.; Liston, D.; Liu, X.; Martin, B. A.; Nelson, R. B.; Nolan, C. E.; Oborski, C. E.; Parker, C. P.; Richter, K. E. G.; Pozdnyakov, N.; Sahagan, B. G.; Schachter, J. B.; Sokolowski, S. A.; Tate, B.; Wood, D. E.; Wood, K. M.; Van Deusen, J. W.; Zhang, L. Design, synthesis, and in vivo characterization of a novel series of tetralin amino imidazoles as γ -secretase inhibitors: Discovery of PF-3084014. *Bioorg. Med. Chem. Lett.* **2011**, *21*, 2637–2640. (m) Churcher, I.; Behr, D.; Best, J. D.; Castro, J. L.; Clarke, E. E.; Gentry, A.; Harrison, T.; Hitzel, L.; Kay, E.; Kerrad, S.; Lewis, H. D.; Morentin-Gutierrez, P.; Mortishire-Smith, R.; Oakley, P. J.; Reilly, M.; Shaw, D. E.; Shearman, M. S.; Teall, M. R.; Williams, S.; Wrigley, J. D. J. 4-Substituted cyclohexyl sulfones as potent, orally active γ -secretase inhibitors. *Bioorg. Med. Chem. Lett.* **2006**, *16*, 280–284.
- (7) (a) Siemers, E. R.; Dean, R. A.; Friedrich, S.; Ferguson-Sells, L.; Gonzales, C.; Farlow, M. R.; May, P. C. Safety, tolerability, and effects on plasma and cerebrospinal fluid amyloid- β after inhibition of γ -secretase. *Clin. Neuropharmacol.* **2007**, *30*, 317–325. (b) Mayer, S. C.; Krefit, A. F.; Harrison, B.; Abou-Gharbia, M.; Antane, M.; Aschmies, S.; Atchison, K.; Chlenov, M.; Cole, D. C.; Comery, T.; Diamantidis, G.; Ellingboe, J.; Fan, K.; Galante, R.; Gonzales, C.; Ho, D. M.; Hoke, M. E.; Hu, Y.; Huryn, D.; Jain, U.; Jin, M.; Kremer, K.; Kubrak, D.; Lin, M.; Lu, P.; Magolda, R.; Martone, R.; Moore, W.; Oganessian, A.; Pangalos, M. N.; Porte, A.; Reinhart, P.; Resnick, L.; Riddell, D. R.; Sonnenberg-Reines, J.; Stock, J. R.; Sun, S.-C.; Wagner, E.; Wang, T.; Woller, K.; Xu, Z.; Zaleska, M. M.; Zeldis, J.; Zhang, M.; Zhou, H.; Jacobsen, J. S. Discovery of Begacestat, a notch-1-sparing γ -secretase inhibitor for the treatment of Alzheimer's disease. *J. Med. Chem.* **2008**, *51*, 7348–7351. (c) Gillman, K. W.; Starrett, J. E.; Parker, M. F.; Xie, K.; Bronson, J. J.; Marcin, L. R.; McElhone, K. E.; Bergstrom, C. P.; Mate, R. A.; Williams, R.; Meredith, J. E.; Burton, C. R.; Barten, D. M.; Toyn, J. H.; Roberts, S. B.; Lentz, K. A.; Houston, J. G.; Zaczek, R.; Albright, C. F.; Decicco, C. P.; Macor, J. E.; Olson, R. E. Discovery and evaluation of BMS-708163, a potent, selective and orally bioavailable γ -secretase inhibitor. *ACS Med. Chem. Lett.* **2010**, *1*, 120–124. (d) Barten, D. M.; Guss, V. L.; Corsa, J. A.; Loo, A.; Hansel, S. B.; Zheng, M.; Munoz, B.; Srinivasan, K.; Wang, B.; Robertson, B. J.; Polson, C. T.; Wang, J.; Roberts, S. B.; Hendrick, J. P.; Anderson, J. J.; Loy, J. K.; Denton, R.; Verdoorn, T. A.; Smith, D. W.; Felsenstein, K. M. Dynamics of β -amyloid reductions in brain, cerebrospinal fluid, and plasma of β -amyloid precursor protein transgenic mice treated with a γ -secretase inhibitor. *J. Pharmacol. Exp. Ther.* **2005**, *312*, 635–643.
- (8) For a review, see Burkhard, J. A.; Wuitschik, G.; Rogers-Evans, M.; Müller, K.; Carreira, E. M. Oxetanes as versatile elements in drug discovery and synthesis. *Angew. Chem., Int. Ed.* **2010**, *49*, 9052–9067. For examples, see (a) Wuitschik, G.; Carreira, E. M.; Wagner, B.; Fischer, H.; Parrilla, I.; Schuler, F.; Rogers-Evans, M.; Müller, K. Oxetanes in drug discovery: Structural and synthetic insights. *J. Med. Chem.* **2010**, *53*, 3227–3246. (b) Wuitschik, G.; Rogers-Evans, M.; Buckl, A.; Bernasconi, M.; Märki, M.; Godel, T.; Fischer, H.; Wagner, B.; Parrilla, I.; Schuler, F.; Schneider, J.; Alker, A.; Schweizer, W. B.; Müller, K.; Carreira, E. M. Spirocyclic oxetanes: Synthesis and properties. *Angew. Chem., Int. Ed.* **2008**, *47*, 4512–4515. (c) Wuitschik, G.; Rogers-Evans, M.; Müller, K.; Fischer, H.; Wagner, B.; Schuler, F.; Polonchuk, L.; Carreira, E. M. Oxetanes as promising modules in drug discovery. *Angew. Chem., Int. Ed.* **2006**, *45*, 7736–7739.
- (9) Evans, R. D.; Magee, J. W.; Schauble, J. H. Halocyclization of unsaturated alcohols and carboxylic acids using bis(sym-collidine)-iodine(I) perchlorate. *Synthesis* **1988**, 862–868.
- (10) Nerdel, F.; Weyerstahl, P.; Lucas, K. Fragmentation reactions of carbonyl compounds with electronegative substituents in the β -position. XIII. Reaction of nucleophilic agents and β -tosyloxyaldehydes. *Tetrahedron. Lett.* **1968**, *55*, 5751–5754.
- (11) A structurally related analogue was reported previously: Parker, M. F.; Barten, D. M.; Bronson, J. J.; Corsa, J. A.; Dee, M. F.; Gai, Y.; Guss, V. L.; Higgins, M. A.; Keavy, D. J.; Loo, A.; Mate, R. A.; Marcin, L. R.; McElhone, K.; Polson, C. T.; Roberts, S. B. 2-(N-Benzyl-N-phenylsulfonamido)alkyl amide derivatives as γ -secretase inhibitors. Abstracts of Papers, 238th ACS National Meeting, Washington, DC, United States, August 16–20, MEDI-043, 2009.
- (12) Lanz, T. A.; Wood, K. M.; Richter, K. E.; Nolan, C. E.; Becker, S. L.; Pozdnyakov, N.; Martin, B. A.; Du, P.; Oborski, C. E.; Wood, D. E.; Brown, T. M.; Finley, J. E.; Sokolowski, S. A.; Hicks, C. D.; Coffman, K. J.; Geoghegan, K. F.; Brodney, M. A.; Liston, D.; Tate, B. Pharmacodynamics and pharmacokinetics of the γ -secretase inhibitor PF-3084014. *J. Pharmacol. Exp. Ther.* **2010**, *334*, 269–277.
- (13) Lombardo, F.; Shalaeva, M. Y.; Tupper, K. A.; Gao, F. ElogD(oct): A tool for lipophilicity determination in drug discovery. 2. Basic and neutral compounds. *J. Med. Chem.* **2001**, *44*, 2490–2497.
- (14) Callegari, E.; Malhotra, B.; Bungay, P. J.; Webster, R.; Fenner, K. S.; Kempshall, S.; Laperle, J. L.; Michel, M. C.; Kay, G. G. A comprehensive nonclinical evaluation of the CNS penetration potential of antimuscarinic agents for the treatment of overactive bladder. *Br. J. Clin. Pharmacol.* **2011**, *72*, 235–246.
- (15) Busfield, W. K.; Grice, I. D.; Jenkins, I. D. Reactions of tert-butoxyl radicals with cyclic ethers studied by the radical trapping technique. *J. Chem. Soc., Perkin Trans.* **1994**, *2*, 1079–1086.
- (16) Hughes, J. D.; Blagg, J.; Price, D. A.; Bailey, S.; Decrescenzo, G. A.; Devraj, R. V.; Ellsworth, E.; Fobian, Y. M.; Gibbs, M. E.; Gilles, R. W.; Greene, N.; Huang, E.; Krieger-Burke, T.; Loesel, J.; Wager, T.; Whiteley, L.; Zhang, Y. Physicochemical drug properties associated with in vivo toxicological outcomes. *Bioorg. Med. Chem. Lett.* **2008**, *18*, 4872–4875.
- (17) Edwards, M. P.; Price, D. A. Role of physicochemical properties and ligand lipophilicity efficiency in addressing drug safety risks. *Annu. Rep. Med. Chem.* **2010**, *45*, 381–391.
- (18) (a) Wager, T. T.; Chandrasekaran, R. Y.; Hou, X.; Troutman, M. D.; Verhoest, P. R.; Villalobos, A.; Will, Y. Defining desirable central nervous system drug space through the alignment of molecular properties, in vitro ADME, and safety attributes. *ACS Chem. Neurosci.* **2010**, *1*, 420–434. (b) Wager, T. T.; Hou, X.; Verhoest, P. R.; Villalobos, A. Moving beyond rules: the development of a central nervous system multiparameter optimization (CNS MPO) approach to enable alignment of druglike properties. *ACS Chem. Neurosci.* **2010**, *1*, 435–449.
- (19) Lu, Y.; Zhang, L.; Nolan, C. E.; Becker, S. L.; Atchison, K.; Robshaw, A. E.; Pustilnik, L. R.; Osgood, S. M.; Miller, E. H.; Stepan, A. F.; Subramanyam, C.; Efremov, I.; Hallgren, A. J.; Riddell, D. Quantitative Pharmacokinetic/Pharmacodynamic Analyses Suggest That 129/SVE Mouse Is A Suitable Preclinical Pharmacology Model For Identifying Small Molecule Gamma Secretase Inhibitors. *J. Pharmacol. Exp. Ther.* **2011**, DOI: 10.1124/jpet.111.186791.
- (20) The observations on the differences in metabolic stability between rodent and human are not surprising considering that species differences in CYP-mediated metabolism are well-established. This can lead to pronounced differences in in vivo pharmacokinetics between the two species. See (a) Naritomi, Y.; Terashita, S.; Kimura, S.; Suzuki, A.; Kagayama, A.; Sugiyama, Y. Prediction of human hepatic clearance from in vivo animal experiments and in vivo metabolic studies with liver microsomes from animals and humans. *Drug Metab. Dispos.* **2001**, *29*, 1316–1324. (b) Cao, X.; Gibbs, S. T.; Fang, L.; Miller, H. A.; Landowski, C. P.; Shin, H.-C.; Lennernas, H.; Zhong, Y.; Amidon, G. I.; Yu, L. X.; Sun, D. Why is it challenging to predict intestinal drug absorption and oral bioavailability in human using rat model. *Pharm. Res.* **2006**, *23*, 1675–1686.